Electron tunneling in heavily In-doped polycrystalline CdS films

M. V. Garcia-Cuenca, J. L. Morenza, and J. Esteve

Departamento de Electricidad y Electrónica, Facultad de Física, Universidad de Barcelona, Diagonal 647, Barcelona 28, Spain

The electrical properties of heavily In-doped polycrystalline CdS films have been studied as a function of the doping level. The films were prepared by vacuum coevaporation of CdS and In. Conductivity and Hall measurements were performed over the temperature range 77–400 K. The conductivity decreases weakly with the temperature and shows a tendency towards saturation at low temperatures. A simple relationship $\sigma = \sigma_0(1 + \beta T^2)$ is found in the low-temperature range. The temperature dependence of the mobility is similar to that of the conductivity since the Hall coefficient is found to be a constant in the whole temperature range. We interpret the experimental results in terms of a modified version of grain-boundary trapping Seto's model, taking into account thermionic emission and tunneling of carriers through the potential barriers. The barriers are found to be high and narrow, and tunneling becomes the predominating transport mechanism.

I. INTRODUCTION

The electrical properties of polycrystalline CdS films have been studied by many workers. Thermally activated mobilities have been reported in undoped[1-4] and doped[5,6] CdS films. Theoretical analysis has been carried out in terms of the model first proposed by Volger[7] and extended by Petritz,[8] Seto,[9] and other authors.[1-4,10,11] According to the grain-boundary trapping theory, free carriers are trapped by trapping states at the grain boundaries, resulting in a depletion region and a potential barrier between grains. On the assumption that current flow is limited by thermionic emission of carriers over the barriers, the mobility is thermally activated with a negative temperature coefficient: $\mu = \mu_0 \exp - (E_a/T)$.

This model has been able to explain most of the electrical properties of polycrystalline semiconductors. However, in CdS, the temperature dependence of the mobility has not been explained well enough. The exponential relationship is not observed; on the contrary, a saturation tendency appears at low temperatures. This behavior has been reported in CdS films prepared by vacuum evaporation,[5,12] spray pyrolysis,[4] and hot-wall epitaxy,[13] and with carrier concentration levels in the 10^{16}–10^{19}-cm^{-3} range. Some authors have related this behavior to the tunneling across the barriers, but no analysis has been done on the contribution of this transport mechanism.

Martinez et al.[14] have developed a model that includes thermionic emission and tunneling through the barriers in polycrystalline Si, with carrier concentrations up to 10^{18} cm^{-3}. Recently, both transport mechanisms have been considered by Seager et al.[15] in the analysis of conduction through GaAs grain boundaries.

In this work we present the results of the electrical conductivity and Hall-effect measurements as a function of temperature for a series of heavily In-doped CdS films. In order to explain these results we develop a modified version of the grain-boundary trapping theory. We restrict Seto's model to the high doping level case and we consider that grain-to-grain transport takes place by thermionic emission and tunneling through the potential barriers.

II. THEORY

We assume, as in Seto's work, that it is sufficient to treat the problem in one dimension. We take into account only the case of high doping level and partial depletion of the crystallite. The conduction-band bottom inside the grain E_C is taken to be at zero energy (Fig. 1).

In the degeneration case (we can take as a validity condition $E_F > 3kT$), the carrier concentration n within the crystallite is related to the Fermi level by

$$E_F = (h^2/2m^*)(3n/8\pi)^{2/3}, \tag{1}$$

where m^* is the conduction-band effective mass and h is Planck's constant.

The abrupt depletion approximation is inappropriate in the degeneration case. If we approximate the Fermi function by its zero temperature limit, $f(E,E_F) = 1$ if $E < E_F$ and $f(E,E_F) = 0$ if $E > E_F$, the carrier concentration in the depletion region is given by

$$n(x) = (n/E_F^{3/2})[E_F - \phi(x)]^{3/2}, \quad -s' < x < 0,$$
$$n(x) = 0, \quad 0 < x < s, \tag{2}$$

where $\phi(x)$ is the energy barrier. s and s' are the widths of the total and partial depletion regions, respectively, and $x = 0$ is
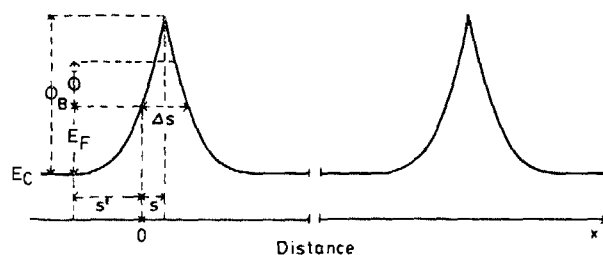

FIG. 1. Energy band diagram of heavily-doped polycrystalline CdS.

defined by the condition $E_F = \phi$ (Fig. 1). Then Poisson's equation becomes

$$\frac{d^2V}{dx^2} = -\frac{qN_D}{\epsilon} + \frac{qn}{\epsilon E_F^{3/2}}(E_F + qV)^{3/2} \quad -s' \leqslant x \leqslant 0 ,$$

(3)

$$d^2V/dx^2 = -(qN_D/\epsilon) \quad 0 \leqslant x \leqslant s ,$$

where N_D is the doping concentration and ϵ is the dielectric permittivity. By integrating and applying the boundary conditions, $V = 0$ and $dV/dx = 0$ at $x = -s'$, V and dV/dx are continuous at $x = 0$, we find the energy barrier:

$$\phi(x) = \frac{q^2 N_D x^2}{2\epsilon} + q\left(\frac{2N_D E_F}{\epsilon} - \frac{4nE_F}{5\epsilon}\right)^{1/2} x + E_F ,$$

(4)

$$0 \leqslant x \leqslant s .$$

At the grain boundary, N_T acceptor trap states become filled. We will assume that N_T is temperature independent. Electrical neutrality requires

$$N_T/2 = s N_D + Q/q ,$$

(5)

where Q is the charge in the partial depletion region, $Q = \epsilon/q(d\phi/dx)_{x=0}$. From Eq. (4) and identifying n with N_D, we obtain

$$Q = (6\epsilon N_D E_F/5)^{1/2} ,$$

(6)

and substituting in Eq. (6),

$$s = \frac{N_T}{2N_D} - \left(\frac{6\epsilon E_F}{5q^2 N_D}\right)^{1/2} .$$

(7)

From Eqs. (4) and (7) the energy barrier height $\phi_B = \phi(s)$ is given by

$$\phi_B = \frac{q^2 N_T^2}{8\epsilon N_D} + \frac{2E_F}{5} .$$

(8)

We consider that the transport through the barriers takes place mainly by thermionic emission and tunneling. The total current can be expressed as

$$J = J_1 + J_2 ,$$

(9)

where J_1 and J_2 are the current densities associated with each transport mechanism.

When the voltage applied to the crystallite is low enough, i.e., $qV \ll kT$, the thermionic emission current density is[16]

$$J_1 = \left(A^* T^2 \exp -\frac{\phi_B - E_F}{kT}\right)\frac{qV}{kT} ,$$

(10)

where $A^* = 4\pi q m^* k^2/h^3$ is the effective Richardson constant. V is the voltage applied to the crystallite on the assumption that the voltage drop in the grain bulk is negligible compared with the voltage drop in the barrier. Since the Fermi level is located inside the conduction band, this expression may not be valid. We can take as a validity condition $\phi_B - E_F > 3kT$.

A suitable expression of the tunneling current density J_2, in the case shown in Fig. 1, is that calculated by Simmons[17,18] in terms of the WKB approximation, for the tunneling current between two similar electrodes through a potential barrier of arbitrary shape. If

$$\bar{\phi} = \frac{1}{\Delta s}\int_0^{\Delta s} [\phi(x) - E_F] \, dx$$

is the mean barrier height above the negatively biased electrode Fermi level, and Δs the barrier width at Fermi level, the tunneling current density at 0 K and low-voltage bias $qV \ll \bar{\phi}$ can be expressed as

$$J_0 = V\frac{q^2(2m^*)^{1/2}\bar{\phi}^{1/2}}{h^2\Delta s}\exp -\frac{4\pi(2m^*)^{1/2}\Delta s \bar{\phi}^{1/2}}{h} , \quad (11)$$

and at any other temperature,

$$J_2 = J_0 \left[FT/\sin(FT)\right] ,$$

(12)

where

$$F = \frac{2\pi^2(2m^*)^{1/2}k\Delta s}{h\bar{\phi}^{1/2}} .$$

(13)

For very low voltages, $\bar{\phi}$ can be considered to be the zero-voltage mean barrier and $\Delta s = 2s$. From Eqs. (4) and (7) we find

$$\bar{\phi} = \frac{q^2 N_T^2}{24\epsilon N_D} + \left(\frac{q^2 E_F}{120\epsilon N_D}\right)^{1/2} N_T - \frac{2E_F}{5} .$$

(14)

According to Eq. (9), the film conductivity can be expressed as $\sigma = \sigma_1 + \sigma_2$ and, if L is the grain size,

$$\sigma_1 = LJ_1/V$$

(15)

is the conductivity associated with the thermionic emission current and

$$\sigma_2 = LJ_2/V$$

(16)

is the conductivity associated with the tunneling current. By considering Eqs. (10) and (12) it follows that

$$\sigma = \frac{LqA^*}{k}T\exp\left(-\frac{\phi_B - E_F}{kT}\right) + \sigma_0\frac{FT}{\sin(FT)} , \quad (17)$$

where $\sigma_0 = LJ_0/V_0$ is the limit of the film conductivity at 0 K and from Eq. (11),

$$\sigma_0 = L\frac{q^2(2m^*)^{1/2}\bar{\phi}^{1/2}}{2h^2 s}\exp -\frac{8\pi(2m^*)^{1/2}s\bar{\phi}^{1/2}}{h} . \quad (18)$$

Finally, for values of FT small enough, σ_2 can be expressed as

$$\sigma_2 = \sigma_0[1 + (F^2/6)T^2] .$$

(19)

With regard to the temperature dependence of the mobility, we can consider that if $LN_D \gg N_T$, the average carrier concentration in the whole grain $\bar{n}$ coincides with the carrier concentration n in the bulk.[9] Then, in the degeneration case, the mobility obtained from $\sigma = \mu\bar{n}q$ has the same temperature dependence as the conductivity, because $\bar{n} \approx n$ and n is temperature independent.

III. EXPERIMENTAL DETAILS

The In-doped CdS films were deposited onto glass substrates at 250 °C by coevaporation of In and CdS. The deposition rate was around 15 nm/s. The doping concentrations N_D were obtained from the relative fluxes of CdS and In and range from 8×10^{18} to 2×10^{20} cm^{-3}.

The film thicknesses measured with a profiling stylus are near 1.5 μm. The grain sizes measured on the SEM mi-

TABLE I. Results obtained on six samples with different doping levels (A) by measurements, (B) by application of the model.

	Sample	25-1	25-3	23-1	17-1	12-1	18-1
(A)	$N_D(10^{19}\,cm^{-3})$	0.86	1.1	4.0	4.7	7.4	23
	$\sigma(300\,K)(\Omega^{-1}\,cm^{-1})$	3.20	4.98	68.2	90.7	164	196
	$n(10^{18}\,cm^{-3})$	9.7	15	44	48	56	73
	$\mu(300\,K)(cm^2\,V^{-1}\,s^{-1})$	2.1	2.1	9.8	12	18	17
	$\sigma_0(\Omega^{-1}\,cm^{-1})$	0.656	1.26	46.6	63.6	141	185
	$(6\beta)^{1/2}(10^{-3}\,K^{-1})$	16.1	11.4	5.52	5.30	3.35	2.05
(B)	$N_T(10^{13}\,cm^{-2})$	1.07	1.47	2.96	3.15	3.42	4.19
	$\phi_B(eV)$	0.36	0.45	0.66	0.68	0.70	0.82
	$E_F(eV)$	0.10	0.14	0.28	0.30	0.33	0.39
	$\Delta s(nm)$	6.2	5.3	3.0	2.9	2.5	2.3
	$\bar\phi\,(eV)$	0.11	0.14	0.17	0.18	0.17	0.19
	$F(10^{-3}\,K^{-1})$	10	8.1	4.1	3.8	3.4	2.9
	$\sigma_1(300\,K)(10^{-2}\,\Omega^{-1}\,cm^{-1})$	15	1.8	0.12	0.10	0.17	0.026

crographs are around 500 nm. The films were formed into van der Pauw clover leaf patterns by mechanical removal of unwanted material, and the electrical contacts were prepared by In evaporation.

The samples were mounted in a Dewar-vessel cryostat and Hall-effect and conductivity measurements were made over the temperature range 77–400 K.

IV. RESULTS

A. By measurements

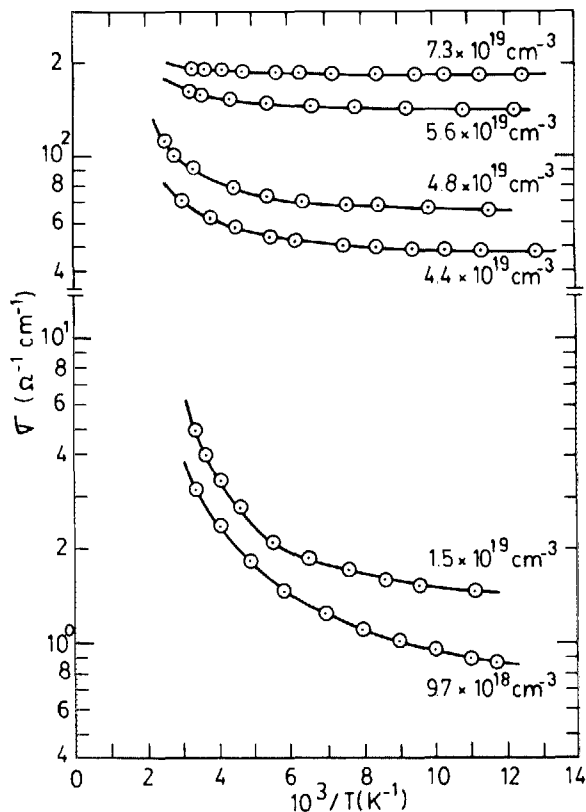Measurements were made on six samples (Table I). The conductivity at 300 K takes values between 3 and 200

FIG. 2. Experimental temperature dependence of the conductivity on six samples with different carrier concentrations.

$\Omega^{-1}\,cm^{-1}$. In all the samples it decreases weakly as temperature decreases and shows a tendency towards saturation at low temperatures. The Arrhenius plots do not show the existence of a thermal activation energy (Fig. 2). However, for each sample there is a linear relationship between the experimental data of σ and T^2 (Fig. 3) over a temperature range that increases with the doping level (around 77–170 K for sample 25-1 and 77–300 K for sample 18-1). (Figure 4 shows the limit of this interval for other samples.)

It has been shown[19] that the Hall measurements give the average concentration $\bar n$ in the crystallite if the intergrain region has a negligible width and a much lower conductivity than the grain region. So we calculate $\bar n$ from the experimental Hall data as $\bar n = (q|R_H|)^{-1}$. $\bar n$ is constant over the whole temperature range in all the samples. It takes values between 10^{19} and $7 \times 10^{19}\,cm^{-3}$ depending on the doping level and, except for the most heavily doped sample, it was found to be $\bar n = N_D \pm 25\%$.

The mobility μ has values at 300 K between 2 and 20 $cm^2\,V^{-1}\,s^{-1}$ and, $\bar n$ being temperature independent, its temperature dependence coincides with that of the conductivity.
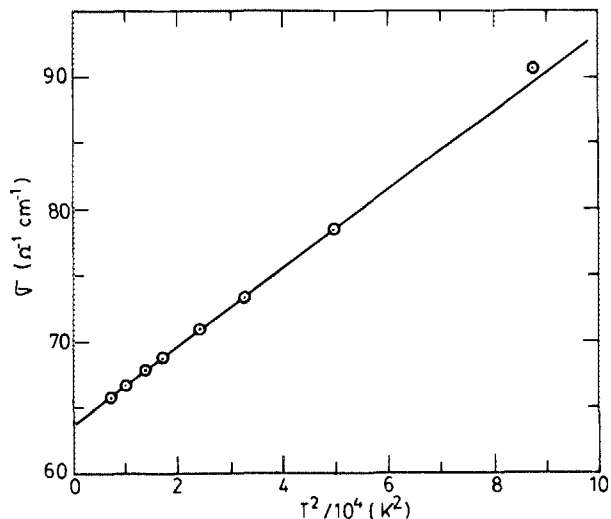

FIG. 3. Experimental data of conductivity as a function of T^2 on the sample 17-1 in Table I. Points fit a relationship $\sigma = \sigma_0(1 + \beta T^2)$ in the low temperature range.

B. By application of the model

1. The conductivity at 0 K

As we have pointed out, the conductivity experimental data fits a relationship $\sigma = \sigma_0(1 + \beta T^2)$ over a wide temperature range, and so we identify σ_0 with the conductivity at 0 K of the theory.

In our samples with grain sizes around 500 nm and high doping level, we expected $LN_D \gg N_T$ and therefore $\bar{n} = n$. This last statement has been experimentally verified, as $\bar{n}$ measured by Hall effect differs from N_D less than the N_D experimental error (and in the grain bulk n must be equal to N_D). This allows us to identify $\bar{n}$ with n in Eq. (1) and with N_D in Eqs. (7) and (14).

By introducing Eq. (1) in Eqs. (7) and (14), and these in the expression of σ_0 Eq. (18), and taking $m^* = 0.16\, m_{e^-}$,[20] we obtain an equation with N_T as the only unknown parameter. In Table I the obtained values of N_T are summarized.

2. The temperature dependence of the conductivity

The conductivity as a function of temperature is only dependent on n and N_T. Since N_T has been determined from σ_0, we make use of the other experimental parameter β in the verification of the theoretical results that, calculated from n and N_T, are summarized in Table I: ϕ_B [Eq. (8)], E_F [Eq. (1)], Δs [Eq. (7)], $\bar{\phi}$ [Eq. (14)], F [Eq. (13)], and σ_1 at 300 K [Eq. (15)].

The thermionic conductivity is only appreciable at the highest temperatures and lowest doping levels (cf. σ_1 at 300 K in Table I), so the calculated total conductivity is practically the conductivity associated with the tunnel effect, except at the highest temperature ranges.

With regard to the tunneling conductivity, σ_2 can be expressed as $\sigma_2 = \sigma_0(1 + F^2 T^2/6)$ if FT is small enough. With the calculated values of F we can take this expression as valid, at least over the low temperature ranges (the error is lower than 20% at 150 K for sample 25-1 and lower than 1% at 300 K for sample 18-1). Therefore, F and $(6\beta)^{1/2}$ should coincide. In Table I the values of these parameters are summarized.

V. DISCUSSION

The obtained values of n and N_T, and therefore, those of ϕ_B and E_F, are consistent with the hypothesis that $LN_D \gg N_T$ and with the applicability conditions of the theory $E_F > 3kT$, $\phi_B - E_F > 3kT$, and $\bar{\phi} > kT$ (obviously, $\bar{\phi} \gg qV$, since $qV \ll kT$).

Also, in all the samples, $E_F < 0.5\,\phi_B$ and so the WKB method is a suitable approximation in this case.

We have assumed that the mobility is limited by the intergrain barriers. Surface scattering is expected to be insignificant for degenerate films with thicknesses around 1.5 μm,[3,21] so the electrical properties of the film are controlled by the bulk. We have neglected the contribution of the grain bulk to the resistivity. We believe that this is a valid approximation in our case for two reasons: first, the mobility temperature dependence is similar to that reported by other authors on CdS films, whose mobilities are limited by the barriers; second, our measured mobilities are much lower
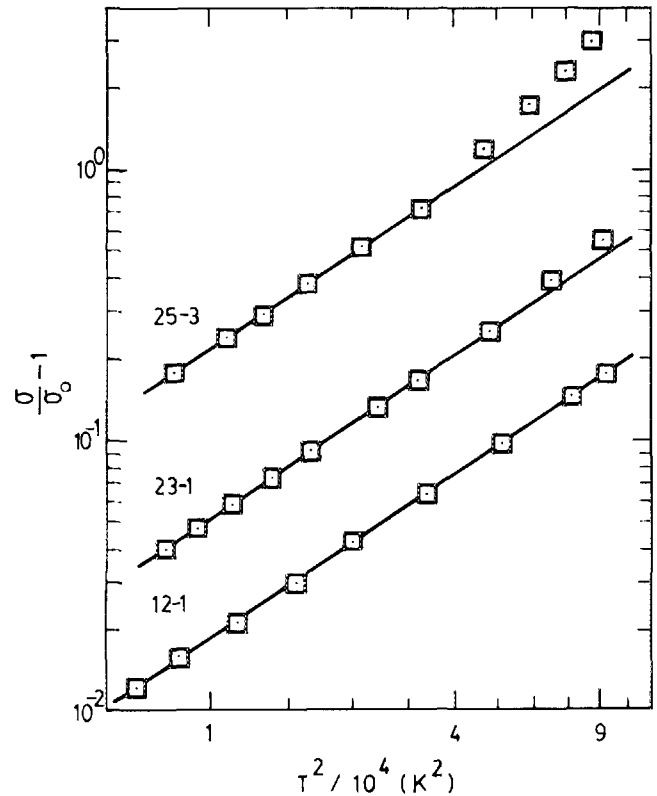

FIG. 4. Experimental values of $(\sigma/\sigma_0) - 1$ plotted against T^2 for samples 25-3, 23-1, and 12-1 in Table I. The linear relationship is observed in a temperature range that increases with the doping level.

than the reported ones[22-24] on monocrystalline CdS, that are around 300 cm^2 V^{-1} s^{-1} at 300 K and higher at lower temperatures.

There is agreement between the values of N_T determined from the tunneling conductivity and the reported ones determined by considering thermionic emission in the transport in polycrystalline semiconductors. The N_T values agree also with the reported value N_{ss} for the surface states density in CdS-metal junctions (in Ref. 25, $N_{ss} = 1.6 \times 10^{13}$ cm^{-2} eV^{-1}).
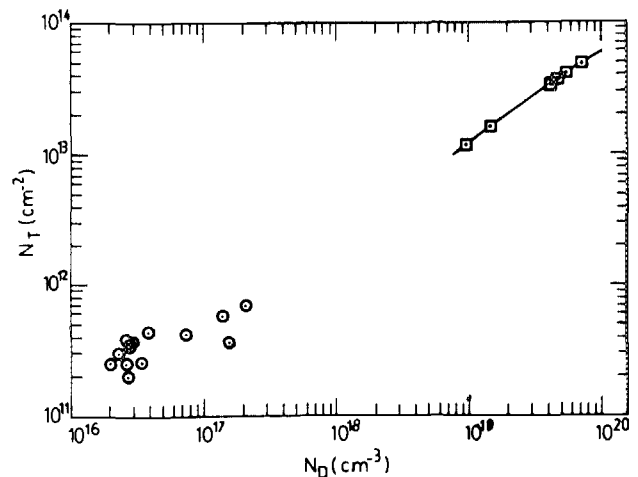

FIG. 5. Trap-states density N_T against doping level N_D. Our results are represented as □, the results of Orton et al. are represented as ⊙.
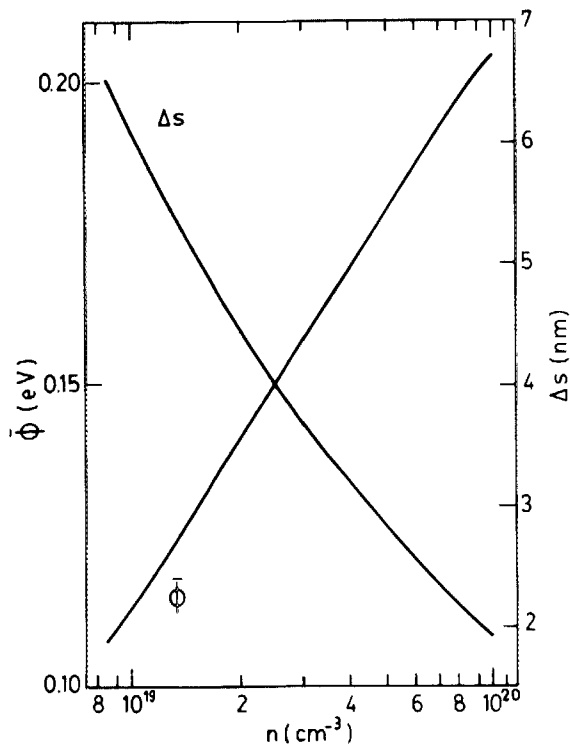
FIG. 6. Barrier width at Fermi level Δs and mean barrier height above Fermi level $\bar{\phi}$ as a function of carrier concentration.

The reasonable values of N_T determined from σ_0 involve high and narrow barriers for the doping levels here considered. From these values of N_T the theoretical results are that the contribution of the thermionic emission is small and, at least in the low temperature range, the conductivity is only the tunneling conductivity and it is a linear function of T^2. The agreement between these results and the experimental data is encouraging, since the σ-T quadratic function is observed experimentally in a temperature range that coincides approximately with the theoretical one (defined by the F value) and the values of F and $(6\beta)^{1/2}$ coincide in order of magnitude for all the samples. Nevertheless, since F and $(6\beta)^{1/2}$ are not equal, there is no one value of N_T that can fit
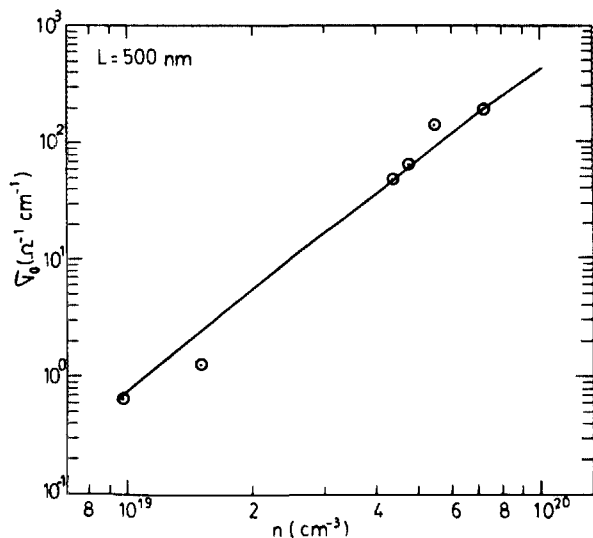

FIG. 7. Solid line is the calculated conductivity at 0 K. Experimental data is represented as ⊙.

σ_0 and β simultaneously. In theory, the density of filled trap states has been considered temperature independent. Actually, N_T determined from σ_0 is its zero temperature limit. Therefore, perhaps a more accurate analysis could be obtained by considering that the density of filled trap states can be temperature dependent. On the other hand, for the two most lightly doped samples, the σ-T quadratic function is observed experimentally in a temperature range larger than that consistent with Eq. (18) for the β value.

N_T increases when the doping level increases. Figure 4 shows N_T plotted against N_D together with the results obtained by Orton et al.[4] on undoped polycrystalline CdS films. A close correlation can be observed in spite of the different doping level. Regarding the dependence of N_T on N_D we can consider two cases[10,11,26]: (a) A monoenergetic density N_{ss} (units of area^{-1}) of trap states. At zero temperature limit the density of filled states N_T will be N_{ss}. (b) A continuous energy distribution of states with a mean density N_{ss} (units of area$^{-1}\times$energy^{-1}). When the doping level is increased, $E_F - \phi_B$ decreases, according to Table I. Therefore, in any case if N_T increases it would be considered that it is because the density of trap states N_{ss} increases when the doping level increases.

From the empirical relationship shown in Fig. 4, we have calculated as a function of n the values Δs, $\bar{\phi}$ (Fig. 5), and σ_0 (Fig. 6). We see that the mean barrier height $\bar{\phi}$ increases when the carrier concentration increases; simultaneously, the barrier width Δs decreases. This effect is dominant, therefore σ_0 increases, F decreases, and the conductivity is more weakly dependent on temperature for the highest carrier concentrations.

VI. CONCLUSION

The grain-boundary trapping theory is applicable to the heavily-doped polycrystalline CdS films if the tunneling current through the potential barrier is considered.

The conductivity of the films is a linear function of T^2 at the low temperature range. This behavior appears because tunneling is the predominant transport mechanism at the low temperature range.

The trap-states density and the 0 K conductivity increase when the doping level increases. The temperature variation of the tunneling conductivity and the contribution of the thermionic conductivity decrease; therefore, for the highest carrier concentrations, grain-to-grain transport at room temperature takes place mainly by tunnel effect, and σ at 300 K tends to σ at 0 K.

ACKNOWLEDGMENTS

[1]J. Dresner and F. V. Shallcross, J. Appl. Phys. **34**, 2390 (1963).
[2]A. Waxman, V. E. Henrich, F. V. Shallcross, H. Borkan, and P. K.

Weimer, J. Appl. Phys. **36**, 168 (1965).

[3]L. L. Kazmerski, W. B. Berry, and C. W. Allen, J. Appl. Phys. **43**, 3515 (1972).

[4]J. W. Orton, B. J. Goldsmith, J. A. Chapman, and M. J. Powell, J. Appl. Phys. **53**, 1602 (1982).

[5]S. Ray, R. Barnejee, and A. K. Barua, Thin Solid Films **87**, 63 (1982).

[6]J. C. Joshi, B. K. Sachar, and P. Kumar, Thin Solid Films **88**, 189 (1982).

[7]J. Volger, Phys. Rev. **79**, 1023 (1950).

[8]R. L. Petritz, Phys. Rev. **104**, 1508 (1956).

[9]J. Y. W. Seto, J. Appl. Phys. **46**, 5247 (1975).

[10]G. Baccarini, B. Ricco, and G. Spadini, J. Appl. Phys. **49**, 5585 (1978).

[11]C. H. Seager and T. G. Catsner, J. Appl. Phys. **49**, 3879 (1978).

[12]S. Ray, R. Barnejee, and A. K. Barua, Jpn. J. Appl. Phys. **19**, 1889 (1980).

[13]J. Humenberger, M. Sadeghi, E. Gruber, G. Elsinger, H. Sitter, and A. Lopez-Otero, J. Phys. Paris **43**, CS-405 (1982).

[14]J. Martinez and J. Piqueras, Solid-State Electron. **23**, 297 (1980).

[15]C. H. Seager and G. E. Pike, Appl. Phys. Lett. **40**, 471 (1982).

[16]S. M. Sze, *Physics of Semiconductor Devices* (Wiley, New York, 1981).

[17]J. G. Simmons, J. Appl. Phys. **34**, 1793 (1963).

[18]J. G. Simmons, J. Phys. D **4**, 613 (1971).

[19]J. Heleskivi and T. Salo, J. Appl. Phys. **43**, 740 (1972).

[20]B. Ray, *II-VI Compounds* (Pergamon, Oxford, 1969).

[21]J. C. Anderson, Adv. Phys. **19**, 311 (1970).

[22]H. H. Woodbury, Phys. Rev. B **9**, 5188 (1974).

[23]L. D. Partain, G. J. Sullivan, and C. E. Birchenall, J. Appl. Phys. **50**, 551 (1979).

[24]P. C. Marthur, B. R. Sethi, P. K. Goyal, and O. P. Sharma, J. Appl. Phys. **52**, 7237 (1981).

[25]A. M. Cowley and S. M. Sze, J. Appl. Phys. **36**, 3212 (1965).

[26]A. K. Ghosh, A. Rose, H. P. Maruska, T. Feng, and D. J. Eustace, J. Electron. Mater. **11**, 237 (1982).